Coherent blue emission generated by Rb two-photon excitation using diode and femtosecond lasers

2017 J. Phys. B: At. Mol. Opt. Phys. 50 085001

(http://iopscience.iop.org/0953-4075/50/8/085001)

IOP Publishing Journal of Physics B: Atomic, Molecular and Optical Physics
J. Phys. B: At. Mol. Opt. Phys. **50** (2017) 085001 (5pp) https://doi.org/10.1088/1361-6455/aa636d

Coherent blue emission generated by Rb two-photon excitation using diode and femtosecond lasers

Jesus P Lopez[1], Marco P Moreno[2], Marcio H G de Miranda[1] and Sandra S Vianna[1]

[1] Departamento de Física, Universidade Federal de Pernambuco, 50670-901 Recife, PE, Brazil
[2] Departamento de Física, Universidade Federal de Rondônia, 76900-726 Ji-Paraná, RO, Brazil

E-mail: vianna@ufpe.br

Received 12 November 2016, revised 21 February 2017
Accepted for publication 28 February 2017
Published 23 March 2017

Abstract

The coherent blue light generated in rubidium vapor due to the combined action of an ultrashort pulse train and a continuous wave diode laser is investigated. Each step of the two-photon transition 5S–$5P_{3/2}$–5D is excited by one of the lasers, and the induced coherence between the 5S and $6P_{3/2}$ states is responsible for generating the blue beam. Measurements of the excitation spectrum reveal the frequency comb structure and allow us to identify the resonant modes responsible for inducing the nonlinear process. Further, each resonant mode excites a different group of atoms, making the process selective in atomic velocity. The signal dependency on the atomic density is characterized by a sharp growth and a rapid saturation. We also show that for high intensity of the diode laser, the Stark shift at resonance causes the signal suppression observed at low atomic density.

Keywords: coherent optical effects, four-wave mixing, rubidium vapor, frequency comb

(Some figures may appear in colour only in the online journal)

1. Introduction

Nonlinear interactions of light and atoms can be enhanced dramatically through the generation of quantum coherence among atomic states. In particular, atomic coherence effects have been explored in four-wave mixing to produce efficiently frequency up-conversion using either low power continuous wave (cw) lasers [1–3] or pulsed lasers [4, 5]. Previous investigations demonstrated the high temporal coherence of the collimated blue light generated in Rb vapor [2] and the ability to transfer orbital angular momentum between the pump and generated beams [6–8]. The interest in these investigations includes quantum information processing and memory [9], photon correlation effects [10, 11] and tunable coherent sources [12].

In this work, we investigate the effects of the two-photon combined interaction of a cw laser and a mode-locked (fs) laser in an Rb vapor for the generation of coherent blue light. The two co-propagating beams, at 780 nm (cw) and 776 nm (fs), drive each step of the two-photon transition $5S_{1/2} \rightarrow 5P_{3/2} \rightarrow 5D$, respectively (see inset of figure 1 (b)). The induced coherence among $5S_{1/2} \rightarrow 5P_{3/2} \rightarrow 5D \rightarrow 6P_{3/2}$ transitions produces, by parametric four-wave mixing (PFWM), a coherent beam at 420 nm [1, 3, 7]. Under the coherent accumulation condition, where the atomic relaxation times are greater than the fs laser repetition period, we show that each individual mode of the frequency comb contributes to the nonlinear signal. The signature of this behavior is the observation of the frequency comb structure in the excitation spectrum of the coherent light, allowing us to identify the resonant modes responsible for the generation of a blue beam with a frequency determined by the parametric process.

The role of each mode of the frequency comb in the two-photon transition of Rb vapor has been investigated using direct frequency comb spectroscopy [13, 14] or similar experimental schemes, with diode (cw) and mode-locked (fs) beams in a co- and contra-propagating configurations, but detecting the fluorescence at 90° [15, 16]. In both cases, the detected signal has its origin in a spontaneous emission

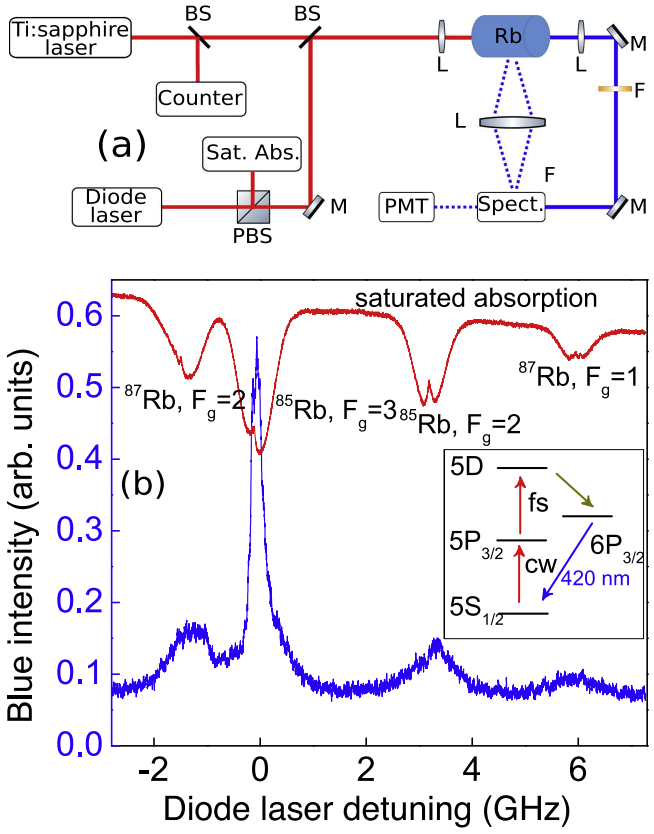

Figure 1 (a) Experimental setup. (b) Excitation spectrum of the blue light emission as a function of the diode frequency for the D_2 Doppler lines at $T = 85$ °C and $I_{cw} = 1.9$ W cm^{-2}. This curve is the average of two scans. The saturated absorption signal (upper curve) is detected simultaneously. The inset shows the relevant energy levels of Rb for the PFWM process. Zero detuning is chosen at the ^{85}Rb, 5S, $F_g = 3 \rightarrow 5P_{3/2}$, $F = 4$ transition.

process and reflects the population of the excited state 5D. In the PFWM process investigated here, the nonlinear signal is determined by two-photon coherence between the 5S and 5D states, and by the amplified spontaneous emission at 5.2 μm [17]. In this case, the generated blue light reflects not only the characteristics of the atomic system, but also carries the phase information related with the excitation beams.

This letter is divided into four sections. In section 2, we briefly describe the experimental setup. The results and the theoretical model are discussed in section 3. Finally, in section 4 we present our conclusions.

2. Experimental setup

The experimental setup is depicted in figure 1(a). A diode laser, stabilized in temperature and with a linewidth of about 1 MHz, is used to excite the $5S_{1/2} \rightarrow 5P_{3/2}$ transition. A train of pulses generated by a mode-locked Ti:sapphire laser (MIRA, Coherent) can excite both $5S_{1/2} \rightarrow 5P_{3/2}$ and $5P_{3/2} \rightarrow 5D$ transitions. The two co-propagated beams, with parallel linear polarizations, are focused in a 5 cm long sealed Rb vapor cell. The vapor cell is heated up to ≈100 °C and contains both ^{85}Rb and ^{87}Rb isotopes in their natural abundances. We measure the dependence on the Rb density of the coherent blue light generated in the forward direction for different diode laser intensities. The measurements were performed as a function of the diode frequency allowing us to realize a velocity-selective spectroscopy [18, 19].

The Ti:sapphire laser with a repetition rate of $f_R \approx 76$ MHz produces 100 fs pulses and 500 mW of average power spread over an ≈10 nm bandwidth, corresponding to about 10^5 modes. The optical frequency of mode m is given by the comb equation $f_m = mf_R + f_0$, where f_0 is the carrier-envelope offset frequency [13]. The fs laser intensity was kept fixed with a mode intensity (the ratio between the average femtosecond laser intensity and the number of modes within its bandwidth) of order of 1 mW cm^{-2} in the cell entrance. The diode laser can sweep over 10 GHz by tuning its injection current and a saturated absorption setup is used to calibrate its frequency. The diameter of the two beams is almost constant inside the cell and it is about 400 μm for the fs beam and 260 μm for the diode laser. The blue beam generated at 420 nm is collected in the forward direction, satisfying the phase-matching condition in the PFWM process. Bandpass filters and a spectrometer, placed about 1.0 m from the cell, are used to cut the light around 780 nm. The signal is detected with a photomultiplier tube and recorded on a digital oscilloscope.

3. Results and discussion

3.1. Excitation spectrum

Figure 1(b) shows the blue signal intensity (lower curve) as the diode frequency is scanned over the four Doppler-broadened D_2 lines of the ^{85}Rb and ^{87}Rb. The origin of the horizontal scale was arbitrarily chosen at the $5S_{1/2}$, $F_g = 3 \rightarrow 5P_{3/2}$, $F = 4$ transition of the ^{85}Rb. The spectrum consists of one sharp and intense peak over a weak broad peak together with other three weak broad peaks, all over a flat background. The intense peak is due to the PFWM process when the two-photon transition is excited by both lasers: the diode laser and the fs laser. The weak broad peaks are the blue fluorescence induced by both lasers; while the flat background is due only to the excitation by the fs laser [14]. The spectrum was obtained for cell temperature of 85 °C and diode intensity of $I_{cw} = 1.9$ W cm^{-2}. The saturated absorption curve (upper curve) is used to calibrate the diode frequency. In figure 2 we display the excitation spectra when the generated signal is detected after an analyzer. We have also included an inset with the blue fluorescence detected at 90°. From these spectra, it is clear that while the fluorescence is not polarized, the intense peak due to the PFWM process practically disappears when the polarization of the incident beams and the analyzer are perpendicular, indicating that this signal is generated with the same polarization of the incident beams [20]. This polarization behavior is also a demonstration that the blue emission has its origin in the nonlinear process. Another important feature to be reinforced here is the directionality of the generated emission that is detected by more than 1 m from the cell.

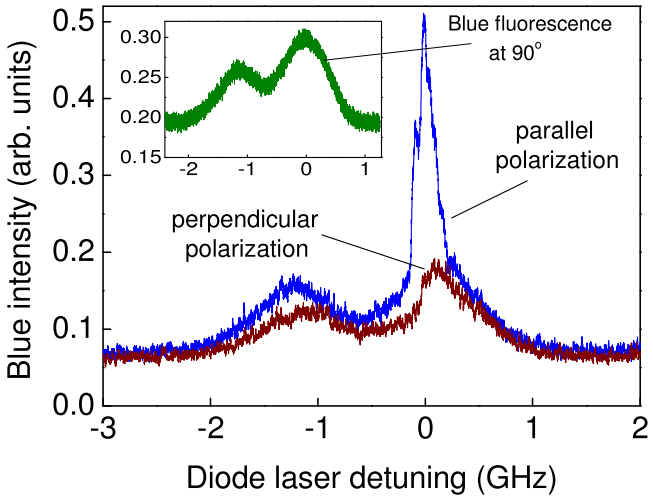

Figure 2. Blue light intensity as a function of the diode frequency for two analyzer polarizations: parallel (blue curve) and perpendicular (red curve) to the incident beams polarization, at $T = 85$ °C and $I_{cw} = 1.9$ W cm^{-2}. The inset shows the blue fluorescence detected at 90°. The peak in the parallel polarization verifies the PFWM process.

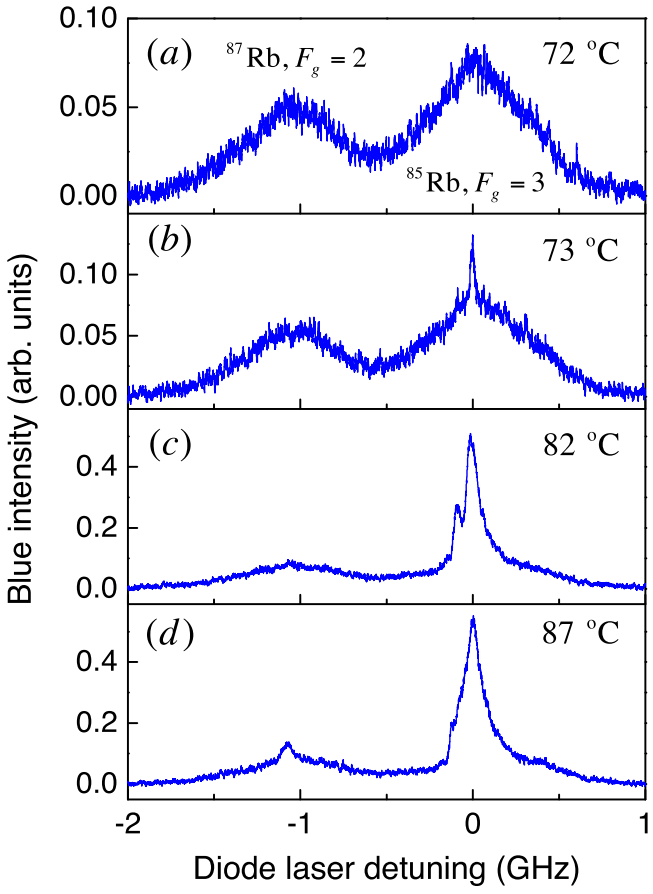

Figure 3. Excitation spectrum of the blue light emission as a function of the diode frequency for different temperatures. $I_{cw} = 1.9$ W cm^{-2} and $I_{fs} = 1.0$ mW cm^{-2} (each mode). The flat background was removed.

The blue signal for different Rb vapor temperatures is shown in figure 3 for the Doppler lines $F_g = 3$ of ^{85}Rb and $F_g = 2$ of ^{87}Rb when the diode laser intensity is fixed at $I_{cw} = 1.9$ W cm^{-2}. For comparison, the flat background has been removed. We note from figures 3(a) and (b) that, for ^{85}Rb, the threshold of the PFWM process occurs between 72 °C and 73 °C. The critical dependence of the PFWM signal on the atomic density is revealed when only one mode of the frequency comb contributes to the signal. This mode is close to the resonance with the cyclic transition for the atomic velocity group that has the highest density.

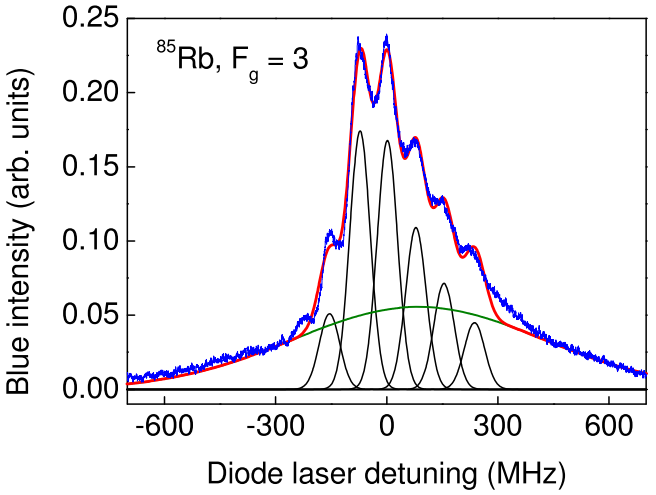

Figure 4. Blue light intensity (blue line) and fit curves (red, green and black lines) as a function of the diode laser frequency, at $T = 85$ °C. The red line is the sum of the fluorescence contribution (green curve) and the contribution of the six modes to the PFWM signal (black lines). The blue curve is the average of 10 measurements.

By increasing temperature other velocity groups reach the threshold of the atomic density, making possible more modes to contribute to the PFWM signal. In figure 3(c) we can distinguish the signal due to two modes of the frequency comb. At higher temperatures, the threshold for the ^{87}Rb density is reached, as showed by the thin peak near -1 GHz in figure 3(d). Under these conditions, we notice in figure 3(d) that the mode structure for the ^{85}Rb appears blurred due to saturation of the atomic density for the intensity of the beams used, along with a rapid scanning of the diode laser, resulting in a broad line. This line shape is similar to the one obtained when two diode lasers are tuned to the maximum of the blue light power [17]. This critical atomic density dependence explains why it is so difficult to observe the comb structure in the PFWM signal, when compared with the fluorescence signal [16].

In order to better understand the role played by the frequency comb in the PFWM process, we focus our attention on the generated signal from the $F_g = 3$ line of the ^{85}Rb, and perform a slow scanning of the diode frequency (taking into account the temporal resolution of the detector) with an average of 10 measurements. The blue curve in figure 4 illustrates the result obtained. The experimental parameters are similar to those used in figure 3 with $T = 85$ °C. We fit the experimental data with a superposition of Gaussian curves in order to quantify the separation between the peaks. The green line is a Gaussian curve that fits the weak broad peak of the fluorescence, with a Doppler width of order of 500 MHz; while the black curves that fit the PFWM signal are also

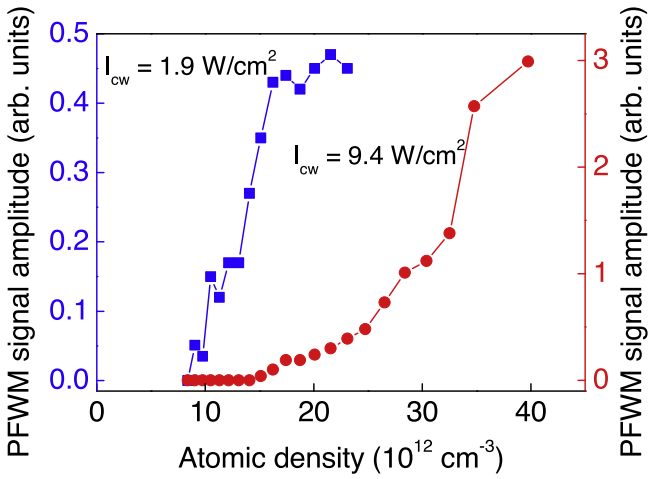

Figure 5. Amplitude of the PFWM signal in the Doppler line $F_g = 3$ of ^{85}Rb as a function of the atomic density, for two diode laser intensities.

Gaussians, all with the same linewidth, ≈55 MHz, but dislocated in frequency. The red line is the sum of all Gaussian curves. The frequency difference between two adjacent black peaks is 78 ± 4 MHz, which is close to the $f_R \approx 76$ MHz of the fs laser; moreover, the linewidth of the black curves are certainly enlarged by power broadening and the jitter of the optical frequency of each mode. Although the jitter of the repetition rate (δf_R) is of order of few Hz, the jitter of the optical frequency of mode m (δf_m) is given by $\delta f_m = \delta f_R\,(f_m/f_R)$, corresponding to tens of MHz. We also notice an atomic density saturation for the peaks near the cycle transition frequency (center of the scan in figure 4). The experimental result (blue curve), together with the Gaussian curves fit (red curve), indicate that the observed peak structure is a clear contribution of each resonant frequency mode to the induced coherence in the vapor, which is responsible for generating the coherent blue light. Each mode excites a different group of atoms, making the process selective in atomic velocity, and being responsible by the modulation observed in the excitation spectra shown in figure 4.

3.2. Atomic density and diode intensity dependence

The results presented above indicate the existence of a sharp growth and a saturation of the PFWM signal as the atomic density increases. To characterize this atomic density dependence we first separate the different contributions to the blue signal by using the same procedure described in the previous subsection. Thereby, we fit each spectrum with different Gaussian curves, in order to separate the fluorescence of each peak related with the PFWM process. This allows us to get the amplitude of the PFWM signal, for a determined diode frequency, as a function of the atomic density, as shown in figure 5, for two diode intensities: $I_{cw} = 1.9$ W cm^{-2} (blue squares) and $I_{cw} = 9.4$ W cm^{-2} (red circles), with a mode intensity of order of $I_{fs} = 1.0$ mW cm^{-2}. For $I_{cw} = 1.9$ W cm^{-2}, we see a threshold-like behavior at $\approx 9 \times 10^{12}$ cm^{-3} and a saturation at $\approx 18 \times 10^{12}$ cm^{-3}, while for $I_{cw} = 9.4$ W cm^{-2} these atomic densities change to $\approx 15 \times 10^{12}$ cm^{-3} and $\approx 40 \times 10^{12}$ cm^{-3}, respectively. This

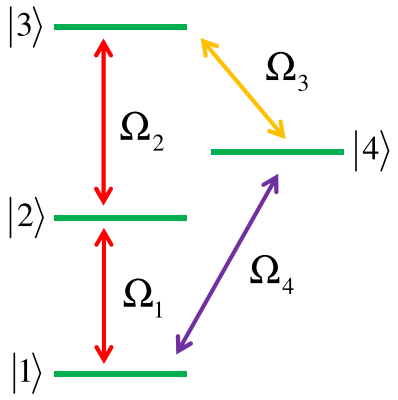

Figure 6. Schematic representation of the electric dipole interactions of the diamond-type four-level system with the four cw fields.

threshold-like atomic density behavior is very similar to that observed using only cw diode lasers [17], and beyond which the regime of exponential gain predicted by the up-conversion PFWM process [21] is established. However, for a fix incident power, further increasing the atomic density causes the system to cross to a saturation regime. On the other hand, for high diode laser intensities, the Stark shift at resonance can inhibit the two-photon excitation process, leading to the suppression of the coherent signal at low atomic density, as observed in figure 5. However, the strong absorption of the 780 nm light allow us to recover the signal as the atomic density increases.

The main observed features, the threshold-like behavior followed by a exponential gain and then a saturation, together with the suppression of the signal at high diode intensities, can be described modeling the interaction of a diamond-type four-level system with four coherent cw fields, as showed by figure 6. We consider the interaction Hamiltonian in the electric dipole approximation,

$$\hat{H}_{\rm int} = -\hbar \sum_{j \neq k}^{4} (\Omega_j(z,\,t) e^{i\omega_j t} + \text{c.c.}) |j\rangle\langle k|, \tag{1}$$

where $\Omega_j(z,\,t)$ and ω_j are the Rabi frequency of the transition indicated in figure 6 and the optical frequency of the fields, and write the Maxwell–Bloch equations as follow:

$$\frac{\partial \rho_{jk}(z,\,t)}{\partial t} = -(i\omega_{jk} + \gamma_{jk})\rho_{jk}(z,\,t) - \frac{i}{\hbar}\langle j|[\hat{H}_{\rm int},\,\hat{\rho}]|k\rangle, \tag{2a}$$

$$\frac{\partial \Omega_j(z,\,t)}{\partial z} = -i\alpha_{jk}\gamma_{jk}\sigma_{jk}(z,\,t). \tag{2b}$$

In these equations, γ_{jk} is the lifetime of the density matrix element ρ_{jk}, ω_{jk} is the frequency of the $j \rightarrow k$ transition and $\sigma_{jk} = \rho_{jk} e^{-i\omega_j t}$ (with $j \neq k$). α_{jk} is the coupling coefficient defined as

$$\alpha_{jk} = \frac{\mu_{jk}^2 \omega_j}{2\hbar c \epsilon_0 \gamma_{jk}} N, \tag{3}$$

where μ_{jk} is the electric dipole moment of the $j \rightarrow k$ transition and N is the atomic density.

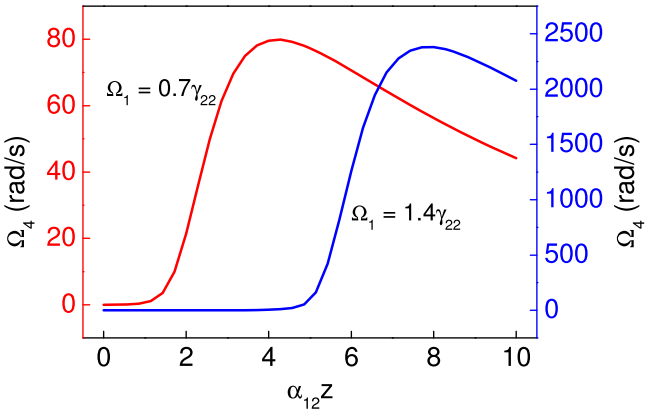

Figure 7. Rabi frequency of the generated field, Ω_4, as a function of the optical depth, $\alpha_{12}z$, for two different values of Ω_1.

We use this theoretical model to describe the behavior of the coherent blue signal as a function of the atomic density. The results are represented in figure 7, for two intensity values of the field that drives the first transition, Ω_1, corresponding to the diode laser. The Rabi frequency of the generated field, Ω_4, is calculated numerically using the fourth order Runge–Kutta method, with the conditions $\delta_j = \omega_{jk} - \omega_j = 0$, $\rho_{11}(z, 0) = 1$, $\rho_{ij}(z, 0) = 0$ for $\{i, j\} \neq \{1, 1\}$, $\Omega_1(0, 0) = \Omega_1$, $\Omega_2(0, 0) = 2.4\gamma_{33}$, $\Omega_3(0, 0) = 2.4 \times 10^{-7}\gamma_{33}$ and $\Omega_4(0, 0) = 0$. The initial value to Ω_3 is necessary to start the four-wave mixing process and then to generate the blue beam (Ω_4). The equations were integrated with step sizes of $0.01\alpha_{12}^{-1}$ in the z axis and 5 ps in the time, over 300 ns.

The curves in figure 7 are for a specific atomic velocity group, which is resonant with the four fields. This situation corresponds to the experimental conditions of the results presented in figure 5, where the coherent signal is observed for a fixed diode laser frequency in which an atomic velocity group is resonant with both: the diode laser and one mode of the frequency comb. Although this theoretical model does not take into account effects like optical pumping to other hyperfine levels or Kerr lensing, we see a good agreement between experiment and numerical calculations. In particular, we find how the combination of high diode intensity and the absorption effects can modify the generation of the coherent blue signal. Moreover, the decrease of the Rabi frequency of the generated field in the saturation regime (high optical depth), as indicate in figure 7, is caused by absorption of either the 780 nm light of the cw laser and/or the blue generated signal, followed by fluorescent light.

4. Conclusions

In conclusion, we have investigated the coherent blue light generated in atomic Rb vapor using a PFWM process due to the combined action of a cw laser and a train of ultrashort pulses. The frequency comb, that drives the upper transition, behaves like a set of cw diode lasers with different frequencies, and the atomic system interacts resonantly with a few of them, resulting in an excitation selective of different atomic velocity groups. Each resonant mode is responsible for inducing the nonlinear process, and the atomic density dependence of the generated signal is characterized by a sharp growth and a rapid saturation. We have also verified, for high diode laser intensities, the suppression of the coherent signal at low atomic density due to the Stark shift at resonance. Remarkably, scanning only the diode laser we can generate several blue beams, each one from a different atomic velocity group with its blue frequency determined by the PFWM process. Studies of the spectral and temporal characteristics of the blue emission are in development. Another feature to be explored is the fixed phase relation between the modes of the frequency comb and the possibility to transfer this phase relation to the generated beams.

Acknowledgments

This work was supported by CNPq, FACEPE and CAPES (Brazilian Agencies).

References

[1] Zibrov A S, Lukin M D, Hollberg L and Scully M O 2002 *Phys. Rev.* A **65** 051801
[2] Meijer T, White J D, Smeets B, Jeppesen M and Scholten R E 2006 *Opt. Lett.* **31** 1002
[3] Brekke E and Alderson L 2013 *Opt. Lett.* **38** 2147
[4] Efthimiopoulos T, Movsessian M E, Katharakis M and Merlemis N 1996 *J. Appl. Phys.* **80** 639
[5] Ariunbold G O, Kash M M, Sautenkov V A, Li H, Rostovtsev Y V, Welch G R and Scully M O 2011 *J. Opt. Soc. Am.* B **28** 515
[6] Walker G, Arnold A S and Franke-Arnold S 2012 *Phys. Rev. Lett.* **108** 243601
[7] Akulshin A M, McLean R J, Mikhailov E E and Novikova I 2015 *Opt. Lett.* **40** 1109
[8] Akulshin A M, Novikova I, Mikhailov E E, Suslov S A and McLean R J 2016 *Opt. Lett.* **41** 1146
[9] Cai Y, Feng J, Wang H, Ferrini G, Xu X, Jing J and Treps N 2015 *Phys. Rev.* A **91** 013843
[10] McCormick C F, Boyer V, Arimondo E and Lett P D 2007 *Opt. Lett.* **32** 178
[11] Willis R T, Becerra F E, Orozco L A and Rolston S L 2011 *Opt. Express* **19** 14632–41
[12] Akulshin A, Perrella C, Truong G-W, McLean R and Luiten A 2012 *J. Phys. B: At. Mol. Opt. Phys.* **45** 245503
[13] Barmes I, Witte S and Eikema S E K 2013 *Phys. Rev. Lett.* **111** 023007
[14] Vujičić N, Ban T, Kregar G, Aumiler D and Pichler G 2013 *Phys. Rev.* A **87** 013438
[15] Moreno M P, Nogueira G T, Felinto D and Vianna S S 2012 *Opt. Lett.* **37** 4344–6
[16] Lira F A, Moreno M P and Vianna S S 2015 *J. Phys. B: At. Mol. Opt. Phys.* **48** 245001
[17] Akulshin A M, McLean R J, Sidorov A I and Hannaford P 2009 *Opt. Express* **17** 22861–70
[18] Aumiler D, Ban T, Skenderović H and Pichler G 2005 *Phys. Rev. Lett.* **95** 233001
[19] Moreno M P and Vianna S S 2011 *J. Opt. Soc. Am.* B **28** 2066–9
[20] Kienlen M B *et al* 2013 *Am. J. Phys.* **81** 442–9
[21] Boyd R W 2003 *Nonlinear Optics* 2nd edn (New York: Academic)